Changes in the fractal dimension on peri-implant trabecular bone after loading : a retrospective study

Teh-Jing Mu

The Graduate School

Yonsei University

Department of Dental Science

Changes in the fractal dimension on peri-implant trabecular bone after loading : a retrospective study

Directed by Professor Ik-Sang Moon

A Master's Thesis

submitted to the Department of Dentistry

and the Graduate School of Yonsei University

in partial fulfillment of the requirements for the degree of

Master of Dental Science

Teh-Jing Mu

June 2012

This certifies that the Master's thesis

of Teh-Jing Mu is approved.

Thesis Supervisor: Ik-Sang Moon

Thesis Committee Member#1 : Kwang-Ho Park

Thesis Committee Member#2 : Dong-Won Lee

The Graduate School

Yonsei University

June 2012

감사의 글

치주학을 전공하고자 교수님을 만나 뵙던 그 순간이 아직 기억속에 생생합니다. 부족한 저를 가르쳐 주시고 이 논문이 완성되기까지 항상 자상한 지도와 격려로 이끌어주신 문익상 지도교수님께 깊은 감사와 존경의 마음을 드립니다. 교수님의 학문에 대한 열정과 지식을 가슴 깊이 간직하고 어느곳에서나 부족하지만 청출어람 할 수 있는 제자가 될 수 있도록 최선을 다해 노력하겠습니다. 아울러 바쁜 와중에도 심사 과정동안 부족한 저의 논문을 검토해주신 박광호 교수님과 논문 작성의 이론과 방법에 대해 지도해주신 이동원 교수님께도 감사드립니다.

병원 생활, 학교생활의 모든것의 길잡이가 되어준 남대호, 이동원 선생님, 3 년 내내 동거동락한 손선보 선생님, 그리고 많이 도와주지 못해 항상 미안한 우리 이청운, 어연호, 최재용, 송소란 선생님 모두와의 추억도 가슴깊이 남아있습니다.

그리고 아무 걱정없이 공부할 수 있도록 늘 제 뒤를 든든히 후원해주시는 사랑하는 부모님과 언니들, 그리고 막내 동생처럼 예뻐해주는 형부들, 귀여운 조카 모두와 기쁨을 나누겠습니다.

2012 년 6 월

모덕경

TABLE OF CONTENTS

LEGEND OF FIGURES

LEGEND OF TABLES

ABSTRACT

Changes in the fractal dimension on peri-implant trabecular bone after loading : a retrospective study

Teh-jing Mu, D.D.S.

Department of Dental Science
The Graduate School, Yonsei University

(Directed by Professor Ik-Sang Moon, D.D.S., M.S.D., Ph.D.)

The aim of this study was to assess bony trabecular changes caused by loading stress around dental implants using fractal dimension analysis. Forty eight subjects (23 males and 25 females; age range: 33 to 77 years; mean age: 58 years) were selected from patients who were treated with dental implants for replacement of missing teeth at the Department of Periodontology, Gangnam Severance Dental Hospital between Januay 2007 and December 2010. Seventy-two internal-hexed implants (AstraTech Osseospeed^{TM}, Astra Techs Dental Implant System; Astra Tech AB, Mölndal, Sweden) were used.

Fractal dimension was measured by comparing radiographs taken immediately after prosthesis delivery to those taken one year after functional loading. Regions of interest were cropped, and a fractal analysis was performed using the box-counting method of

ImageJ 1.42 software. Wilcoxon's signed-rank test was used to analyze the differences in before and after delivery.

The mean fractal dimension before loading (1.4213 ± 0.0525) increased significantly to 1.4329 ± 0.0479 at 12 months after loading ($p < 0.05$). Our results demonstrated that more increased fractal dimensions after loading, which could suggest an increased amount of bony microstructure around the implant. It may be concluded that there is an adaptive remodeling response of the surrounding bone to functional loading. Fractal dimension analysis might be helpful to detection of changes of peri-implant alveolar trabecular bone pattern in clinical situation.

Key words: fractal dimension, dental implant, loading

Changes in the fractal dimension on peri-implant trabecular bone after loading : a retrospective study

Teh-Jing Mu, D.D.S.

Department of Dentistry

The Graduate School, Yonsei University

(Directed by Professor Ik-Sang Moon, D.D.S., M.S.D., Ph.D.)

I. INTRODUCTION

Dental implants are ankylosed to surrounding bone without the periodontal ligament. Trabecular bone around an implant thus plays major roles in supporting the functional pressure exerted by the implant and in dispersing stress by forming a load transfer path (Matsunaga et al. 2010). The key factor for successful implant treatment is the manner in which stresses are transferred to the surrounding bone (Van Staden et al. 2006). Bone tissue undergoes continuous cycles of resorption and formation, and the associated combination of modeling and remodeling is critical to the ability to maintain the stability of the bone–implant interface after loading (Stanford & Brand 1999). Although the precise mechanisms are not fully understood, the surrounding bone clearly shows an adaptive remodeling response to this stress. Finite element analysis (FEA) allows researchers to predict stress around the apices of implants in trabecular bone under various conditions (Geng et al. 2004; Mellal et al. 2004; Li et al. 2007; Chou et al. 2008). However, most FEA models assume a state of optimal osseointegration; thus, another method is needed to detect density distribution around loaded implants *in vivo*.

Periapical radiographs are frequently taken during routine dental examination. These radiographs are traditionally interpreted by measuring peri-implant marginal bone loss, but this most commonly used method has low sensitivity (Åkesson et al. 1992) and has been shown to be of limited diagnostic value for the early detection of changes in bone (Lang & Hill 1977). Digital subtraction radiography is a considerably more sensitive diagnostic method then conventional radiographic interpretation (Jeffcoat et al. 1992), but the high demand of patient positioning reproducibility is a major drawback of this technique (Gröndahl et al. 1983).

Fractal analysis, a non-invasive tool that can be used to describe biological systems in clinical studies, is a method of identifying scale-invariant structure that is not affected by exposure or minor alignment variations on radiographs (Lynch et al. 1991a, 1991b; Buckland-Wright et al. 1994; Fazzalari & Parkinson 1998). It is thus well suited to the analysis of trabecular bone patterns on radiographs. Trabecular bone has a branching pattern that exhibits fractal properties, such as self-similarity and lack of a well-defined scale. Thus, the application of fractal geometry and the measurement of fractal dimensions can be used to determine trabecular complexity and bone structure (Chappard et al. 2001).

Several studies have found a strong correlation between the demineralization of alveolar bone and decreasing fractal dimensions (Majumdar et al. 1993; Caligiuri et al. 1994; Wilding et al. 1995; Southard & Southard 1996; Southard et al. 1996). Southard et al. (1996) hypothesized that the radiographic intensity surface would become smoother during demineralization, causing a corresponding reduction in the fractal dimension. Fractal dimensional changes accompanied by changes in bony microstructure have been observed under various conditions. Fractal analysis of dental radiographs has been used to assess osteoporosis (Caligiuri et al. 1994; Law et al. 1996), hyperparathyroidism (Ergün et al. 2009), and changes in periapical trabecular patterns after root canal treatment (Chen et al. 2005; Southard et al. 1996); and to characterize the periodontally compromised population (Shrout et al. 1998; Updike & Nowzari 2008).

Changes in the magnitude of habitual mechanical stimulation should be accompanied by corresponding changes in osseous structure and the orientation of bony trabeculae (Pauwels 1980; Roberts et al. 1984; Melsen & Lang 2001). Therefore, the aim of this study was to assess bony trabecular changes caused by loading stress around dental implants using fractal dimension analysis.

II. MATERIALS AND METHODS

1. Patient selection

This retrospective study was approved by the Institutional Review Board of Yonsei University. All patients were informed in detail about the study procedures and signed an informed consent form. Forty-eight subjects (23 men, 25 women; age range, 33–77 years; mean age, 58 years) were selected from patients who received dental implants to replace missing teeth at the Department of Periodontology, Gangnam Severance Dental Hospital, between January 2007 and December 2010.

All patients selected for this study had functional prostheses for >12 months. Exclusion criteria were untreated active periodontitis, bruxism/parafunctional habits, poor oral hygiene [modified plaque index (mPI) > 2; Mombelli et al. 1987], bone grafting in conjunction with implant placement, and uncontrolled compromised systemic disease.

2. Implants

Seventy-two internal-hexed implants (Astra Tech OsseoSpeed™, Astra Tech Dental Implant System; Astra Tech AB, Mölndal, Sweden) were used to replace missing teeth. Implant lengths ranged from 8 to 13 mm and diameters ranged from 3.5 to 5.0 mm. The distribution of the installed implants is detailed in Table 1.

Table 1. Distribution of the installed implants according to variables

Variable		Implant data (%)	Variable		Implant data (%)
Gender	Male	53	Length(mm)	8	13
	Female	47		9	57
Arch	Maxilla	42		11	42
	Mandible	58		13	29
Tooth type	Incisor	6	Width(mm)	3.5	8
	Canine	0		4.0	51
	Premolar	17		4.5c	3
	Molar	78		5.0c	32
				5.0	6

c: conical neck design

3. Treatment procedure

A two-stage surgical protocol was used. Second-stage surgeries were performed 6 and 3 months after the first stage for maxillary and mandibular implants, respectively. Prostheses were delivered 3 weeks after the second-stage surgery. Patients were recalled every 6 months for professional plaque control and oral hygiene evaluation.

4. Radiographic examination and evaluation

Radiographs were taken with an extension cone paralleling (XCP) device (Rinn, Elgin, IL, USA) using the parallel cone technique (70 kV, 8 mA, 0.250 s). A 5.5-mm spherical metal bearing was placed to aid length measurement. All films were developed using the same automatic processor (Periomat; Durr Dental, Bietigheim-Bissingen, Germany) according to the manufacturer's instructions. Radiographs were digitized using a digital scanner (GT-12000; EPSON, Nagano, Japan) at an input resolution of 2400 dpi with a grayscale spectrum of 256 shades. Periapical radiographs (Kodak Insight, film speed F; Eastman Kodak Company, Rochester, NY, USA) were taken 1 day after implant placement, immediately before the second-stage surgery, immediately after prosthesis delivery, and 1 year after functional loading.

5. Selection of regions of interest and fractal analysis

The region of interest (ROI) was set to a width of 100 pixels and height of 200 pixels (= 1.0 × 2.0 mm) at the first macrothread around the mesial and distal aspects of each implant. The ROIs avoided crestal bone, neighboring tooth roots and lamina dura, the sinus floor, and other structural entities. Because remodeling is pronounced in bone within 1 mm of an implant (Chen et al. 1993, 1994; Garetto et al. 1995), the ROI was set to a width of 1.0 mm adjacent to the implant–bone interface.

Image processing was performed according to the method described in a previous study (White & Rudolph 1999). Briefly, the ROI was blurred using a Gaussian filter (sigma = 35 pixels, kernel size = 33 × 33). The heavily blurred image was then subtracted from the original, and 128 were added to the result at each pixel location. This generated an image with a mean grayscale value of 128, regardless of its initial intensity. The image was then made binary with a threshold brightness value of 128, and eroded and dilated once to reduce noise. The image of the trabeculae was then inverted and skeletonized. Fractal analysis was performed using the box-counting method. Using imaging software (Image J 1.43u; Wayne Rasband, National Institutes of Health, Bethesda, MD, USA), calibration was performed using the known distance of the spherical metal bearing (5.5 mm). Fractal dimensions were compared using radiographs taken immediately after prosthesis delivery and those taken 1 year after functional loading (Figure 1). Intraobserver agreement on ROI placement was assessed by re-evaluation of all of images twice, with a 3-week interval between viewings.

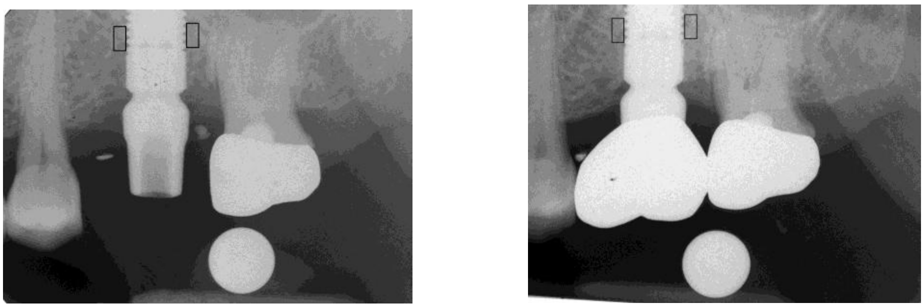

a **b**

Figure 1. ROI was selected (a) immediately after prosthesis delivery; (b) after 1 year.

6. Statistical analysis

The null hypothesis was that there would be no difference in fractal dimensions before and after implant loading. The D'Agostino-Pearson test was used to test the normality of distribution, which was rejected. Thus, the Wilcoxon signed-rank test was used to analyze differences in fractal dimensions before and after loadingimplant delivery. Computer software (MedCalc for Windows, version 11.2.1.0; MedCalc Software, Mariakerke, Belgium.) was used to process the data. The values were deemed statistically significant when $p < 0.05$. The intraobserver agreement reliability was evaluated by calculating Cronbach's alpha coefficients.

III. RESULT

1. Clinical examination

All implants functioned normally and no specific complication was found during the observation period. No subject complained of pain or implant mobility, and no inflammation was observed in any implant. The peri-implant soft tissues were found to be clinically healthy.

2. Fractal dimensions before and after occlusal loading

The Cronbach's alpha value for interobserver reliability was 0.8780. The mean fractal dimension was 1.4213 ± 0.0525 before loading, and increased significantly to 1.4329 ± 0.0479 at 12 months after loading ($p < 0.05$; Table 2, Figure. 2).

Table 2. Fractal dimensional change

	At delivery	After 1yr loading	p- value
Mean ± SD	1.4213± 0.0525	1.4329 ±0.0479	p=0.026
median (95% CI)	1.4305(1.4195-1.4439)	1.4367(1.4289-1.4529)	

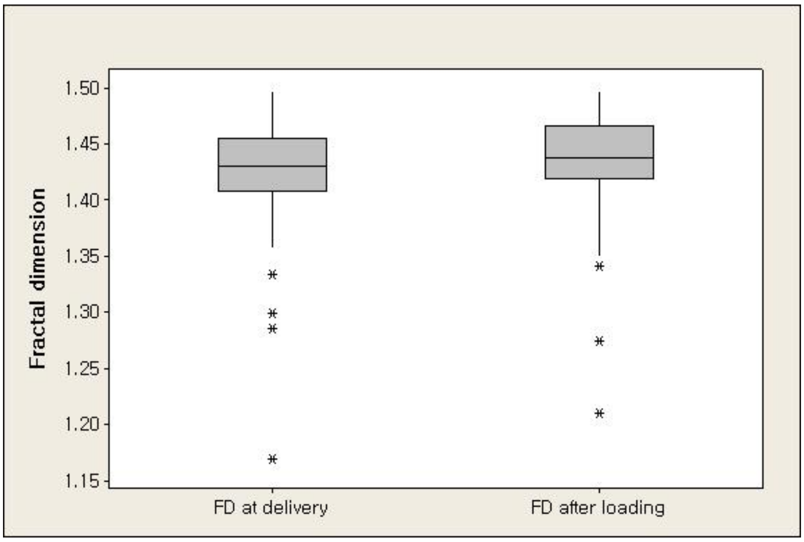

Figure 2. Fractal dimension alteration

IV. DISCUSSION

Implants exposed to functional loading exhibit signs of bone remodeling, including the presence of bone multicellular units (BMUs) and a higher degree of bone–implant contact (Ogiso et al. 1994; Piattelli et al. 1998; Gotfredsen et al. 2001; Berglundh et al. 2005). Mechanical loading also increases the bone volume fraction and trabecular thickness and content, and alters trabecular morphology (Roberts et al. 1984; Fritton et al. 2005; Yamada et al. 2005; Van Der Meulen et al. 2006). The removal and addition of bone matrix by osteoclasts and osteoblasts may transform the trabecular architecture, which has been shown to be an important factor affecting the mechanical properties of bone and is highly correlated with bone strength (Kinney & Ladd 1998; Majumdar et al. 1998).

The analysis of fractal dimensions on periapical radiographs has been used as a simple descriptor of the complex trabecular bone architecture (Ruttimann et al. 1992; Geraets & Van der Stelt 2000). Several studies have assessed the reliability of fractal dimension calculations from radiographs (Southard et al. 1996; Chen & Chen 1998), finding that they are not sensitive to small alignment variations or over- or subexposition. Furthermore, ROI placement has been found to be more critical than ROI size (Jolley et al. 2006; Shrout et al. 1997a, 1997b). In our study, we used standardized periapical radiographs and carefully placed ROIs to minimize the potential unknown effects of these factors.

Fractal dimensions had increased significantly after 12 months of loading ($p < 0.05$), suggesting an increase in the amount of bony microstructure around the implant

(Southard et al. 2000). Our findings are consistent with those of a similar study (Wilding et al. 1995), which found an increased fractal dimension at 2 years after implant placement.

Jung (2005) found no significant fractal dimensional change in the first 6 months after implantation. However, that study used panoramic radiographs, which have a much lower resolution than periapical radiographs that prevents the visualization of finer bony structures (Bollen et al. 2001). Moreover, the author provided no information about loading time because the study was focused on the healing process after implantation.

Not all of our data indicated that loading stress increased fractal dimensions. Three major factors affect bony response around loaded dental implants: mechanical influence, implant design, and implant surface (Bianchi et al. 2005). All implant fixtures (OsseoSpeed; Astra Tech AB) used in the present study had the same surface treatment, implant–abutment interface (conical seal design; Astra Tech AB), and thread characteristics. Thus, external loading stress was the major factor influencing fractal dimensional change. Frost (1987) hypothesized that bone modeling and remodeling would be initiated at a critical strain level; peak load magnitudes exceeding 2500–3500 microstrain led to new bone formation until the increased bone mass reduced strain, whereas disuse atrophy was proposed to occur at peak load magnitudes below 50–200 microstrain. Other investigators have reported similar findings but have proposed different thresholds. Melsen & Lang (2001) found that loading significantly influenced the turnover and density of alveolar bone at magnitudes of 3400–6600 microstrain. In other words, the same amount of stress can result in different amounts of strain in bones with different mechanical properties. Bone remodeling capacity can be affected by age and sex (Fedarko et al. 1992; Palinkas et al. 2010; Parfitt 1993). These factors may explain why some of our data showed decreased fractal dimensional values after loading. To date, the magnitude of force necessary to maintain a balance between disuse atrophy and overload resorption in a normal clinical environment has not been established.

Our study demonstrated that fractal analysis of alveolar bone can quantify the response of trabecular bone to functional loading. To achieve the common use of fractal analysis in routine clinical practice, a consensus must be reached about the most appropriate method of calculating fractal dimensions (Geraets & Van der Stelt 2000). The limitation of this study was the short follow up period, as the amount of peri-implant trabecular bone increases over a period longer than 12 months (Wilding et al. 1995; Lin et al. 2010). Further long-term studies are needed to evaluate the relationship between fractal dimension changes and functional loading.

V. CONCLUSION

In conclusion, the increased fractal dimensions around implants after functional loading indicate an adaptive remodeling response of the surrounding bone. Fractal dimension analysis could be helpful in detecting changes in peri-implant alveolar trabecular bone patterns in clinical situations.

VI. References

1. Åkesson, L., Håkansson, J. & Rohlin, M. (1992) Comparison of panoramic and intraoral radiography and pocket probing for the measurement of the marginal bone level. *Journal of clinical periodontology* **19**: 326-332.
2. Berglundh, T., Abrahamsson, I. & Lindhe, J. (2005) Bone reactions to longstanding functional load at implants: An experimental study in dogs. *Journal of clinical periodontology* **32**: 925-932.
3. Bianchi, A.E., Dolci, G., Jr., Sberna, M.T. & Sanfilippo, S. (2005) Factors affecting bone response around loaded titanium dental implants: A literature review. *J Appl Biomater Biomech* **3**: 135-140.
4. Bollen, A., Taguchi, A., Hujoel, P. & Hollender, L. (2001) Fractal dimension on dental radiographs. *Dentomaxillofacial Radiology* **30**: 270.
5. Buckland-Wright, J., Lynch, J., Rymer, J. & Fogelman, I. (1994) Fractal signature analysis of macroradiographs measures trabecular organization in lumbar vertebrae of postmenopausal women. *Calcified tissue international* **54**: 106-112.
6. Caligiuri, P., Giger, M.L. & Favus, M. (1994) Multifractal radiographic analysis of osteoporosis. *Medical physics* **21**: 503.
7. Chappard, D., Legrand, E., Haettich, B., Chales, G., Auvinet, B., Eschard, J.P., Hamelin, J.P., Basle, M.F. & Audran, M. (2001) Fractal dimension of trabecular bone: Comparison of three histomorphometric computed techniques for measuring the architectural two dimensional complexity. *The Journal of Pathology* **195**: 515-521.
8. Chen, J., Chen, K. & Roberts, W. (1993) The effect of occlusion and orthodontic

force on the stresses around an endosseous implant. *ASME-PUBLICATIONS-BED* **26**: 431-431.

9. Chen, J., Lu, X., Paydar, N., Akay, H. & Roberts, W. (1994) Mechanical simulation of the human mandible with and without an endosseous implant. *Medical engineering & physics* **16**: 53-61.
10. Chen, S. & Chen, C. (1998) The effects of projection geometry and trabecular texture on estimated fractal dimensions in two alveolar bone models. *Dentomaxillofacial Radiology* **27**: 270.
11. Chen, S.K., Oviir, T., Lin, C.H., Leu, L.J., Cho, B.H. & Hollender, L. (2005) Digital imaging analysis with mathematical morphology and fractal dimension for evaluation of periapical lesions following endodontic treatment. *Oral Surgery, Oral Medicine, Oral Pathology, Oral Radiology, and Endodontology* **100**: 467-472.
12. Chou, H.Y., Jagodnik, J.J. & Muftu, S. (2008) Predictions of bone remodeling around dental implant systems. *Journal of biomechanics* **41**: 1365-1373.
13. Ergün, S., Saraçoğlu, A., Güneri, P. & Özpınar, B. (2009) Application of fractal analysis in hyperparathyroidism. *Dentomaxillofacial Radiology* **38**: 281-289.
14. Fazzalari, N.L. & Parkinson, I. (1998) Fractal properties of cancellous bone of the iliac crest in vertebral crush fracture. *Bone* **23**: 53-57.
15. Fedarko, N., Vetter, U., Weinstein, S. & Robey, P.G. (1992) Age-related changes in hyaluronan, proteoglycan, collagen, and osteonectin synthesis by human bone cells. *Journal of cellular physiology* **151**: 215-227.
16. Fritton, J., Myers, E., Wright, T. & Van der Meulen, M. (2005) Loading induces site-

specific increases in mineral content assessed by microcomputed tomography of the mouse tibia. *Bone* **36**: 1030-1038.

17. Frost, H. (1987) Bone “mass” and the “mechanostat”: A proposal. *The anatomical record* **219**: 1-9.
18. Garetto, L.P., Chen, J., Parr, J.A. & Roberts, W.E. (1995) Remodeling dynamics of bone supporting rigidly fixed titanium implants: A histomorphometric comparison in four species including humans. *Implant dentistry* **4**: 235-243.
19. Geng, J., Ma, Q., Xu, W., Tan, K. & Liu, G. (2004) Finite element analysis of four thread form configurations in a stepped screw implant. *Journal of Oral Rehabilitation* **31**: 233-239.
20. Geraets, W. & Van der Stelt, P. (2000) Fractal properties of bone. *Dentomaxillofacial Radiology* **29**: 144-153.
21. Gotfredsen, K., Berglundh, T. & Lindhe, J. (2001) Bone reactions adjacent to titanium implants subjected to static load. *Clinical Oral Implants Research* **12**: 1-8.
22. Gröndahl, H.G., Gröndahl, K. & Webber, R.L. (1983) A digital subtraction technique for dental radiography. *Oral surgery, oral medicine, oral pathology* **55**: 96-102.
23. Jeffcoat, M., Reddy, M., Van Den Berg, H. & Bertens, E. (1992) Quantitative digital subtraction radiography for the assessment of peri-implant bone change. *Clinical Oral Implants Research* **3**: 22-27.
24. Jolley, L., Majumdar, S. & Kapila, S. (2006) Technical factors in fractal analysis of periapical radiographs. *Dentomaxillofacial Radiology* **35**: 393.
25. Jung, Y.H. (2005) Evaluation of peri-implant bone using fractal analysis. *Korean*

Journal of Oral and Maxillofacial Radiology **35**: 121-125.

26. Kinney, J. & Ladd, A. (1998) The relationship between three-dimensional connectivity and the elastic properties of trabecular bone. *Journal of Bone and mineral research* **13**: 839-845.
27. Lang, N.P. & Hill, R.W. (1977) Radiographs in periodonties. *Journal of clinical periodontology* **4**: 16-28.
28. Law, A.N., Bollen, A.M. & Chen, S.S.U.K. (1996) Detecting osteoporosis using dental radiographs: A comparison of four methods. *The Journal of the American Dental Association* **127**: 1734-1742.
29. Li, J., Li, H., Shi, L., Fok, A.S.L., Ucer, C., Devlin, H., Horner, K. & Silikas, N. (2007) A mathematical model for simulating the bone remodeling process under mechanical stimulus. *Dental Materials* **23**: 1073-1078.
30. Lin, D., Li, Q., Li, W., Duckmanton, N. & Swain, M. (2010) Mandibular bone remodeling induced by dental implant. *Journal of biomechanics* **43**: 287-293.
31. Lynch, J., Hawkes, D. & Buckland-Wright, J. (1991a) Analysis of texture in macroradiographs of osteoarthritic knees, using the fractal signature. *Physics in medicine and biology* **36**: 709.
32. Lynch, J., Hawkes, D. & Buckland-Wright, J. (1991b) A robust and accurate method for calculating the fractal signature of texture in macroradiographs of osteoarthritic knees. *Informatics for Health and Social Care* **16**: 241-251.Majumdar, S., Kothari, M., Augat, P., Newitt, D., Link, T., Lin, J., Lang, T., Lu, Y. & Genant, H. (1998) High-resolution magnetic resonance imaging: Three-dimensional trabecular bone

architecture and biomechanical properties. *Bone* **22**: 445-454.

33. Majumdar, S., Weinstein, R.S. & Prasad, R.R. (1993) Application of fractal geometry techniques to the study of trabecular bone. *Medical physics* **20**: 1611.

34. Matsunaga, S., Shirakura, Y., Ohashi, T., Nakahara, K., Tamatsu, Y., Takano, N. & Ide, Y. (2010) Biomechanical role of peri-implant cancellous bone architecture. *The International journal of prosthodontics* **23**: 333.

35. Mellal, A., Wiskott, H., Botsis, J., Scherrer, S. & Belser, U. (2004) Stimulating effect of implant loading on surrounding bone. *Clinical Oral Implants Research* **15**: 239-248.

36. Melsen, B. & Lang, N. (2001) Biological reactions of alveolar bone to orthodontic loading of oral implants. *Clinical Oral Implants Research* **12**: 144-152.

37. Mombelli, A., van Oosten, M.A.C., Schu ¨ rch, E. & Lang N, P. (1987) Themicrobiota associated with successful or failing osseointegrated titanium implants. *Oral Microbiology and Immunology* **2**: 145–151.

38. Ogiso, M., Tabata, T., Kuo, P.T. & Borgese, D. (1994) A histologic comparison of the functional loading capacity of an occluded dense apatite implant and the natural dentition. *The Journal of Prosthetic Dentistry* **71**: 581-588.

39. Palinkas, M., Nassar, M.S.P., Cecílio, F.A., Siéssere, S., Semprini, M., Machado-de-Sousa, J.P., Hallak, J.E.C. & Regalo, S.C.H. (2010) Age and gender influence on maximal bite force and masticatory muscles thickness. *Archives of Oral Biology* **55**: 797-802.

40. Parfitt, A.M. (1993) Bone age, mineral density, and fatigue damage. *Calcified tissue*

international **53**: 82-86.

41. Pauwels, F. (1980) Biomechanics of the locomotor apparatus: Springer.
42. Piattelli, A., Corigliano, M., Scarano, A., Costigliola, G. & Paolantonio, M. (1998) Immediate loading of titanium plasma-sprayed implants: An histologic analysis in monkeys. *Journal of periodontology* **69**: 321.
43. Roberts, W.E., Smith, R.K., Zilberman, Y., Mozsary, P.G. & Smith, R.S. (1984) Osseous adaptation to continuous loading of rigid endosseous implants. *American Journal of Orthodontics* **86**: 95-111.
44. Ruttimann, U.E., Webber, R.L. & Hazelrig, J.B. (1992) Fractal dimension from radiographs of peridental alveolar bone:: A possible diagnostic indicator of osteoporosis. *Oral surgery, oral medicine, oral pathology* **74**: 98-110.
45. Shrout, M., Hildebolt, C. & Potter, B. (1997a) The effect of varying the region of interest on calculations of fractal index. *Dentomaxillofacial Radiology* **26**: 295.
46. Shrout, M.K., Potter, B.J. & Hildebolt, C.F. (1997b) The effect of image variations on fractal dimension calculations. *Oral Surgery, Oral Medicine, Oral Pathology, Oral Radiology, and Endodontology* **84**: 96-100.
47. Shrout, M.K., Roberson, B., Potter, B., Mailhot, J. & Hildebolt, C.F. (1998) A comparison of 2 patient populations using fractal analysis. *Journal of periodontology* **69**: 9.
48. Southard, T.E. & Southard, K.A. (1996) Detection of simulated osteoporosis in maxillae using radiographic texture analysis. *Biomedical Engineering, IEEE Transactions on* **43**: 123-132.

49. Southard, T.E., Southard, K.A., Jakobsen, J.R., Hillis, S.L. & Najim, C.A. (1996) Fractal dimension in radiographic analysis of alveolar process bone1. *Oral Surgery, Oral Medicine, Oral Pathology, Oral Radiology, and Endodontology* **82**: 569-576.

50. Southard, T.E., Southard, K.A. & Lee, A. (2001) Alveolar process fractal dimension and postcranial bone density. *Oral Surgery, Oral Medicine, Oral Pathology, Oral Radiology and Endodontics* **91**: 486–491.

51. Stanford, C.M. & Brand, R.A. (1999) Toward an understanding of implant occlusion and strain adaptive bone modeling and remodeling. *The Journal of Prosthetic Dentistry* **81**: 553-561.

52. Updike, S.X. & Nowzari, H. (2008) Fractal analysis of dental radiographs to detect periodontitis-induced trabecular changes. *Journal of periodontal research* **43**: 658-664.

53. Van Der Meulen, M.C.H., Morgan, T.G., Yang, X., Baldini, T.H., Myers, E.R., Wright, T.M. & Bostrom, M.P.G. (2006) Cancellous bone adaptation to in vivo loading in a rabbit model. *Bone* **38**: 871-877.

54. Van Staden, R.C., Guan, H. & Loo, Y.C. (2006) Application of the finite element method in dental implant research. *Comput Methods Biomech Biomed Engin* **9**: 257-270.

55. White, S.C. & Rudolph, D.J. (1999) Alterations of the trabecular pattern of the jaws in patients with osteoporosis. *Oral Surgery, Oral Medicine, Oral Pathology, Oral Radiology, and Endodontology* **88**: 628-635.

56. Wilding, R.J.C., Slabbert, J.C.G., Kathree, H., Owen, C.P., Crombie, K. & Delport, P.

(1995) The use of fractal analysis to reveal remodeling in human alveolar bone following the placement of dental implants. *Archives of Oral Biology* **40**: 61-72.

57. Yamada, A., YAMAKURA, D. & KISHI, M. (2005) Three-dimensional observation of internal structure of canine mandible by microcomputed tomography-morphometric defferences between loadedand unloaded cancellous bone around implants. *JOURNAL-TOKYO DENTAL COLLEGE SOCIETY* **105**: 577.

국문요약

교합력 적용 후 임플란트 주변 골소주에 대한 프랙탈 값의 변화 : 후향적 연구

모 덕 경, D.D.S
연세대학교 대학원 치의학과

<지도교수: 문 익 상, D.D.S., M.S.D., Ph.D.>

이 연구의 목적은 프랙탈 차원 분석을 이용하여 임플란트 주위 골의 골소주의 변화를 측정하는 것이다.

본 연구를 위해 72개의 임플란트(AstraTech Osseospeed^{TM}, Astra Techs Dental Implant System; Astra Tech AB, Mölndal, Sweden)를 식립한 48명의 환자를 선정하였다.

상부 보철물 연결시의 방사선 사진과 기능적 부하를 가하고 1년 후에 방사선 사진를 촬영하였고, 관심영역은 각 임플란트의 근, 원심 부위에 첫 번째 macrothread 인접 치조골에서 100x200 픽셀 크기로 설정하였다. 교합력 적용 전 프랙탈 차원값은 평균 1.4213± 0.0525, 적용 후 값은 평균 1.4329 ± 0.0479으로 Wilcoxon’s signed-rank test를 이용한 분석 결과 통계학적 유의성을 보였다($p<0.05$).

본 연구의 결과, 임플란트 주위 골소주의 변화를 프랙찰 차원으로 정량적인 분석이 가능함을 알 수 있다. 또한 프랙탈 차원은 임플란트 주위 골소주 변화

를 정량적인 방법으로 측정할 수 있는 비침습적이고 효과적인 방법으로 사용될 수 있을것이다.

핵심 단어: 프랙탈 차원 분석, 임플란트, 하중